Solid-State Synthesis and Characterization of Silver Vanadium Oxide for Use as a Cathode Material for Lithium Batteries

Randolph A. Leising and Esther Sans Takeuchi*

Wilson Greatbatch Ltd., 10,000 Wehrle Drive, Clarence, New York 14031

Received November 23, 1993. Revised Manuscript Received January 26, 1994®

Silver vanadium oxide (SVO, $AgV_2O_{5.5}$) was synthesized for use as a cathode material in lithium/SVO batteries. The material was prepared via the solid-state thermal reaction of a silver-containing precursor and vanadium pentoxide at 500 °C under an air or argon atmosphere. The silver-containing precursors examined in this study were silver nitrate, silver nitrite, silver vanadate, silver oxide, silver carbonate, and silver metal powder. SEM analysis of the SVO products indicated that the surface morphology was similar for each of the samples, with the dimensions of the rodlike particles depending on the form of silver used in the reaction. In addition, the degree of crystallinity of the samples depended strongly on the type of silver used in the reaction, as evidenced by X-ray powder diffraction analysis. All of the samples were analyzed by DSC, chemical analysis, X-ray powder diffraction, resistivity measurements, and electrical discharge tests of Li/SVO test cells. The experimental capacities and pulse power capabilities of the SVO samples prepared under an air atmosphere were all almost identical, while the samples synthesized under an inert atmosphere displayed a significant decrease in delivered capacity and pulse power capability.

Introduction

Silver vanadium oxide (SVO, $AgV_2O_{5.5}$) has been successfully used as a solid-state cathode material in lithium power sources for implantable biomedical devices.[1–5] The Li/SVO battery system is capable of supplying low-level background current to power monitoring circuits, as well as rapidly providing high-current pulses on demand. This combination makes Li/SVO a suitable power source for advanced biomedical devices such as the implantable cardiac defibrillator.[6] Although the application of SVO to lithium battery systems is recent, the preparation of SVO has been known since the 1930s.[7–10] Since that time, the synthesis of SVO has been reported over a wide range of temperatures (400–750 °C) with a number of different silver starting materials.[11] Some of the different forms of silver that have been used for the synthesis of SVO include silver nitrate,[7–10,12–17] silver carbonate,[18–20] silver iodide,[20] silver vanadate,[21,22] silver oxide,[22–28] and silver metal.[20,29–35]

Our interest in the properties of SVO as a cathode material for lithium batteries previously resulted in the study of the effect of synthesis temperature on the physical and electrochemical properties of the material.[36] The temperature of preparation was varied from 320 to 540 °C using silver nitrate and vanadium oxide starting materials. As an expansion of this study, we report here the effect of the silver-containing precursor on the solid-state synthesis of SVO under controlled temperature and atmosphere conditions. This report details the synthesis of SVO using silver nitrate, silver carbonate, silver oxide,

---

® Abstract published in *Advance ACS Abstracts*, March 1, 1994.

(1) Takeuchi, E. S. Proceedings, 40th Annual Conference on Engineering in Medicine and Biology; The Alliance for Engineering in Medicine and Biology: Washington, DC, 1987; Abstract 20.2.

(2) Holmes, C. F.; Keister, P.; Takeuchi, E. S. *Progress in Batteries and Solar Cells*; JEC Press: Cleveland, OH, 1987; p 64.

(3) Takeuchi, E. S.; Keister, P. *Extended Abstracts*, 168th Meeting of the Electrochemical Society, Las Vegas, NV; The Electrochemical Society: Pennington, NJ, 1985; Abstract 125.

(4) Liang, C. C.; Bolster, M. E.; Murphy, R. M. U.S. Patent 4,391,729, 1983.

(5) Liang, C. C.; Bolster, M. E.; Murphy, R. M. U.S. Patent 4,310,609, 1982.

(6) Takeuchi, E. S. Proceedings, 6th Annual Battery Conference on Applications and Advances, Long Beach, CA, 1991; 91BM-1.

(7) Britton, J.; Robinson, M. *J. Chem. Soc.* **1930**, *133*, 2328.

(8) Britton, J.; Robinson, M. *J. Chem. Soc.* **1932**, *135*, 1955.

(9) Britton, J.; Robinson, M. *J. Chem. Soc.* **1933**, *136*, 512.

(10) Carriere, E.; Guiter, H. *C. R. Acad. Sci.* **1937**, *204*, 1339.

(11) Hagenmuller, P. In *Comprehensive Inorganic Chemistry*; Bailar, J. C., Emeleus, H. J., Nyholm, R., Trotman-Dickenson, A. F., Eds.; Pergamon Press: Oxford, 1973; pp 541–601.

(12) Takeuchi, E. S.; Thiebolt, W. C. *J. Electrochem. Soc.* **1988**, *135*, 2691–2694.

(13) Takeuchi, E. S.; Piliero, P. *J. Power Sources* **1987**, *21*, 133–141.

(14) Marti, F. B.; Goyannes, C. B. *An. Fis. Y. Quim.* **1947**, *43*, 921.

(15) Andreikov, E. I.; Volkov, V. L. *Kinet. Katal.* **1981**, *22*, 963–968.

(16) Hui-Liang, Z.; Wei, Z.; Xiang, D.; Xian-Cai, F. *J. Catal.* **1991**, *129*, 426–437.

(17) Vassileva, M.; Andreev, A.; Dancheva, S. *Appl. Catal.* **1991**, *69*, 221–234.

(18) Chakraverty, B. K.; Sienko, M. J.; Bonnerot, J. *Phys. Rev. B* **1978**, *17*, 3781–3789.

(19) Ozerov, R. P. *Russ. J. Inorg. Chem.* **1959**, *4*, 476–479.

(20) Scholtens, B. B. *Mater. Res. Bull.* **1976**, *11*, 1533–1538.

(21) Volkov, V. L.; Fotiev, A. A.; Sharova, N. G.; Surat, L. L. *Russ. J. Inorg. Chem.* **1976**, *21*, 1566–1567.

(22) Crespi, A. M. U.S. Patent 5,221,453, 1993.

(23) Casalot, A.; Pouchard, M. *Bull. Soc. Chim. Fr.* **1967**, 3817–3820.

(24) Raveau, B. *Rev. Chim. Miner.* **1967**, *4*, 729–758.

(25) Fleury, P.; Kohlmuller, R. *C. R. Acad. Sci. Paris* **1966**, *262C*, 475–477.

(26) Wenda, E. *J. Thermal Anal.* **1985**, *30*, 879–887.

(27) Fleury, P. *Rev. Chim. Min.* **1969**, *6*, 819.

(28) Takeuchi, E. S.; Beutel, G. R. Presented at the 17th Northeast Regional Meeting of the American Chemical Society, Rochester, NY, Nov 1987; paper 133.

(29) Andersson, S. *Acta Chem. Scand.* **1965**, *19*, 269–270.

(30) Andersson, S. *Acta Chem. Scand.* **1965**, *19*, 1371–1375.

(31) Takada, K.; Kanbara, T.; Yamamura, Y.; Kondo, S. *Eur. J. Solid State Inorg. Chem.* **1991**, *28*, 533–545.

(32) Scholtens, B. B.; Polder, R.; Broers, G. H. J. *Electrochim. Acta* **1978**, *23*, 483–488.

(33) Van Den Berg, J.; Broersma, A.; Van Dillen, A. J.; Geus, J. W. *Thermochim. Acta* **1983**, *63*, 123–128.

(34) Deschanvres, A.; Raveau, B. *C. R. Acad. Sc. Paris* **1964**, 3553.

(35) Bito, Y.; Ito, S.; Takata, K.; Takahashi, S.; Toyoguchi, Y. U.S. Patent 5,194,342, 1993.

(36) Leising, R. A.; Takeuchi, E. S. *Chem. Mater.* **1993**, *5*, 738–742.

0897-4756/94/2806-0489$04.50/0

Table 1. Differential Scanning Calorimetry Isotherms for Mixtures of Starting Materials

starting materials[a]	isotherms[b] (°C)
$V_2O_5 + AgNO_3$	176 (endo), 212 (endo), 285 (endo), 350 (endo), 463 (endo), 541 (endo), 555 (endo)
$V_2O_5 + AgNO_2$	130 (endo), 177 (endo), 218 (endo), 295 (endo), 340 (exo), 467 (endo), 536 (endo), 556 (endo)
$V_2O_5 + AgVO_3$	272 (endo), 344 (exo), 463 (endo), 533 (endo), 556 (endo)
$V_2O_5 + Ag_2O$	373 (exo), 467 (endo), 534 (endo), 553 (endo)
$V_2O_5 + Ag_2CO_3$	193 (endo), 293 (endo), 373 (exo), 467 (endo), 540 (endo), 552 (endo)

[a] Mole ratio of silver to vanadium = 1:2 in each case. [b] Endo = endothermic peak, exo = exothermic peak.

silver nitrite, silver vanadate, and silver metal powder. In addition, air versus argon synthesis atmosphere was examined. Solid-state physical characterization was performed on all of the materials. These results were analyzed in light of the performance of the materials in Li/SVO batteries to determine the effect of the silver starting material and synthesis atmosphere on the electrochemical properties of the final product.

Experimental Section

Silver vanadium oxide was synthesized from a mixture of vanadium pentoxide with a silver-containing precursor, using a ratio of silver to vanadium of 1:2. The dry mixture was ground with a mortar and pestle and heated to 500 °C for 48 h. The samples were removed after the first 16 h and ground again with a mortar and pestle to ensure adequate mixing of components. The samples were heated under either air or argon atmospheres. The synthesis of SVO in air may favor dissociation and result in mixed valence states for the vanadium compound. However, the synthetic conditions in this study were chosen to mimic conditions which can be scaled-up for an industrial process.

Caution! The decomposition of nitrate and nitrite during SVO synthesis liberates NO_x gas, which is highly toxic. The synthesis of SVO with these components should be performed only in a well-ventilated fume hood.

X-ray powder diffraction spectra of silver vanadium oxide were recorded on a Siemens Diffrac 500 instrument using Cu Kα radiation. Spectra were recorded from 10° to 80° (2θ). Si powder (99.999%, Aldrich Chemical) was used as an internal standard for the samples, where a weighed sample of Si was thoroughly mixed with a known amount of SVO. The amount of Si standard was in the range 3.12–3.66% (wt %) of the entire sample. Integrated peak intensity ratios for the X-ray powder patterns listed in Table 4 are normalized for the actual amount of Si in each sample. SEM micrographs of solid SVO samples were recorded at 1000 magnification using an ISI ABT-55 instrument. Differential scanning calorimetry (DSC) analyses of the SVO samples were obtained using a duPont Instruments TA 2000 DSC/DTA. The samples were analyzed under a purge of argon (120 mL/min) in hermetically sealed Al pans to 600 °C at a heating rate of 20 °C/min. Chemical analysis of the SVO samples dissolved in sulfuric acid was performed via a combination of potassium permanganate titrations and sulfur dioxide reduction of the vanadium components of the materials.[12] Resistivity of silver vanadium oxide was measured via the linear four point method[37] on pellets sintered at 500 °C for 18 h. The pellets contained 1.0 g of SVO, and were pressed under a pressure of 5400 kg/cm^2. The pellets containing SVO synthesized under air were sintered under an air atmosphere, while the pellets containing SVO prepared under argon were sintered under an argon atmosphere. The electrochemical test cell consisted of a single cathode sandwiched between two anodes. The cathode contained 94% silver vanadium oxide, 1% carbon, 2% graphite, and 3% PTFE. The cathode was formed by compressing the mix on a titanium current collector at a pressure of 5400 kg/cm^2. Anodes consisted of lithium metal pressed onto a nickel current collector. Assembly of test cells was performed under a dry air atmosphere. Two layers of polypropylene separator were placed between the cathode and each anode, and the electrodes were held in position by glass plates. The electrode assembly was placed in a glass jar filled with 1 M lithium hexafluoroarsenate in 50/50 by volume propylene carbonate/dimethoxyethane electrolyte. The cell was capped and tested under a constant resistance load of 200 Ω at 25 °C. Pulse power capability was measured on identical test cells, discharged under a constant resistance load of 681 Ω at 25 °C with 18 mA/cm^2 pulse current. The pulse discharge was accomplished using a scheme of four 10-s pulses, with 15-s rest between pulses. Two sets of four pulses were applied each day, ~8 h apart.

Results and Discussion

The silver vanadium oxide samples were prepared by the reaction of vanadium pentoxide with a silver-containing precursor under either an air or argon atmosphere. The temperature of the solid state synthesis was set at 500 °C, based on analysis of DSC curves for 1:1 mixtures of silver and vanadium oxide starting materials. Results for the thermal analysis of these mixtures are given in Table 1. As previously reported,[36] the reaction of $AgNO_3$ with V_2O_5 results in a DSC curve dominated by endotherms associated with the melting of the silver salt and subsequent decomposition of nitrate. A similar curve was recorded for the mixture of $AgNO_2$ and V_2O_5, while the mixture of 0.5 Ag_2O with V_2O_5 displays a strong exothermic peak at 375 °C. This same exotherm is found in the reaction of Ag_2CO_3 with V_2O_5, suggesting that the thermal decomposition of silver carbonate (210 °C) results in the in situ formation of silver oxide in the reaction. The reaction of $AgVO_3$ with V_2O_5 results in a weak exotherm at 340 °C. In addition to these low-temperature isotherms all of the above samples displayed endothermic peaks at 463, 537, and 552 °C. The latter two peaks are assigned to the peritectic and eutectic transitions normally found in $AgV_2O_{5.5}$, and the transition at 463 °C is assigned to a eutectic of $AgV_2O_{5.5}$ and $AgVO_3$.[21] The mixture of silver metal powder and vanadium oxide displayed a featureless curve up to 600 °C, indicating no reaction between the two components during the DSC experiment. However, heating the DSC sample to 500 °C for 2 h prior to the analysis resulted in a DSC curve with endothermic peaks at 463 and 553 °C. These results suggest that SVO is formed when additional heating time is provided but that the reaction of silver metal with vanadium oxide is too slow to be measured on the normal time scale of the DSC experiment.

The surface morphology of the SVO materials was examined by SEM analysis of the samples, and micrographs of selected samples are displayed in Figure 1. The samples synthesized under air from $AgNO_2$, $AgVO_3$, and Ag_2O contained similar rodlike particles on the order of 20–50 μm in length 1–3 μm in diameter. SVO produced from $AgNO_3$ and Ag_2CO_3 under an air atmosphere displayed the same type of particle morphology, along with some flattened particles ~5 μm in width. Last, the sample of SVO produced from silver metal powder under air displayed the largest particle size, consisting of flat plates 3–9 μm in width and 30–100 μm in length. In contrast, a slightly different particle morphology is seen for the SVO samples synthesized under an argon atmo-

---

(37) Runyan, W. R. *Semiconductor Measurements and Instrumentation*; McGraw-Hill: New York, 1976; pp 69–72.

(A) SEM of $AgNO_3$ SVO from Air

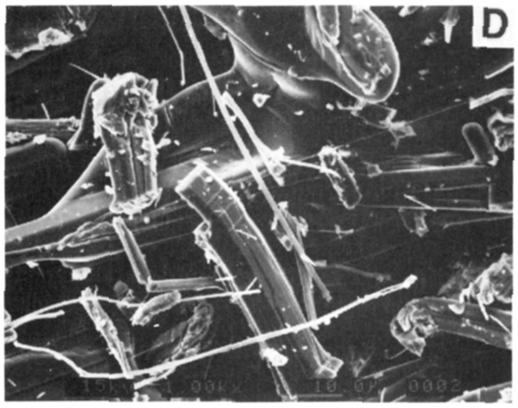

(D) SEM of $AgNO_3$ SVO from Argon

(B) SEM of Ag_2O SVO from Air

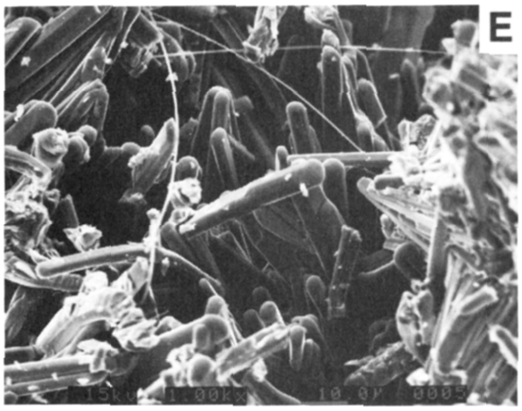

(E) SEM of Ag_2O SVO from Argon

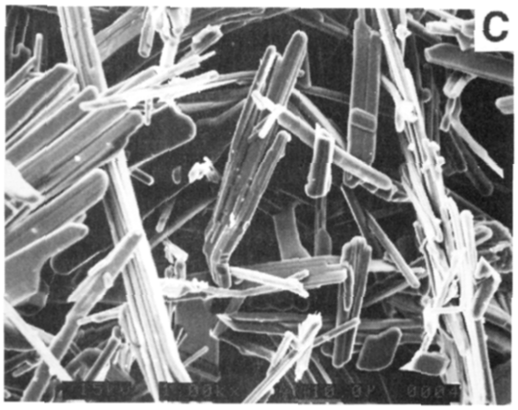

(C) SEM of Ag^0 powder SVO from Air

Figure 1. SEM micrographs (1000× magnification) of (A) $AgNO_3$ SVO (air), (B) Ag_2O SVO (air), (C) Ag^0 powder SVO (air), (D) $AgNO_3$ SVO (argon), and (E) Ag_2O SVO (argon).

sphere. These materials contain larger particles, with a mixture of particle shapes and sizes. The SVO produced from $AgNO_3$ under an argon atmosphere displayed a mixture of large flat plates and thin fiberlike particles with a diameter ~1 μm. Likewise, the SVO resulting from Ag_2O under argon contained rodlike particles (3–4 μm in diameter) along with smaller fragmented particles.

The thermal properties of the SVO products were analyzed using DSC, and regardless of the silver starting material used, all of the samples prepared under an air atmosphere gave identical results. A DSC curve of SVO synthesized from $AgNO_3$ under air, representative of the entire group, is presented in Figure 2. These materials display sharp endothermic transitions at 540 and 552 °C, which are most likely due to a peritectic transformation (527 °C) and eutectic point (545 °C) of $AgV_2O_{5.5}$. The assignments of these peaks are based on the transitions assigned to the composition of $AgV_2O_{5.5}$ in a phase diagram for the mixture of $AgVO_3$ and V_2O_5 reported by Volkov et al.[21] The melting point of $AgV_2O_{5.5}$ is ~640 °C, which is beyond the 600 °C limit of the experiment. In addition to these endotherms, an endothermic shoulder appears at 510 °C and an exothermic peak at 565 °C in these samples. The small peak at 510 °C is unidentified but is also found in SVO synthesized at 540 °C.[36] The exothermic peak may be caused by a crystalline phase change in the material.[38] The SVO materials prepared under an inert atmosphere display DSC curves very different from the samples synthesized under air. The samples synthesized from $AgNO_3$ and Ag_2O under argon produced identical DSC curves, with the curve from the $AgNO_3$-based material

---

(38) Wendlandt, W. W. *Thermal Analysis*; Wiley-Interscience: New York, 1986; pp 215–216.

Table 2. X-ray Powder Diffraction Peaks (*d* Spacings, Intensities) for SVO Samples Prepared under an Air Atmosphere

$AgNO_3$ SVO		$AgNO_2$ SVO		$AgVO_3$ SVO		Ag_2O SVO		Ag_2CO_3 SVO		Ag^0 powder SVO		$Ag_2V_4O_{11}$[a]		$Ag_2V_4O_{11}$[b]	
d (Å)	int	*d* (Å)	int	*d* (Å)	int	*d* (Å)	int	*d* (Å)	int	*d* (Å)	int	*d* (Å)	int	*d* (Å)	int
7.38	30	7.44	50	7.44	40	7.46	50	7.40	30	7.36	20	7.46	60	7.50	60
6.01	20	3.75	50	3.74	60	3.75	40	5.99	30	3.74	20	3.74	30	3.75	70
3.75	30	3.70	60	3.70	60	3.70	40	3.74	60	3.70	80	3.69	30	3.71	30
3.70	60	3.42	30	3.42	30	3.42	50	3.70	60	3.42	5	3.41	60	3.43	70
3.42	10	3.13	70	3.12	40	3.12	40	3.42	40	3.12	10	3.06	80	3.08	70
3.12	20	3.07	90	3.07	100	3.07	90	3.12	30	3.07	30	2.99	80	3.08	70
3.07	80	3.01	100	3.00	100	3.00	90	3.07	100	3.00	40	2.90	100	2.92	100
3.00	70	2.92	100	2.92	80	2.92	100	3.00	90	2.92	10	2.76	80	2.77	80
2.92	30	2.77	80	2.77	80	2.77	90	2.92	100	2.77	10	2.65	30	2.66	40
2.77	40	2.67	30	2.67	20	2.47	60	2.77	90	2.67	5	2.46	30	2.46	40
2.67	10	2.47	70	2.47	70	2.34	50	2.67	20	2.47	100	2.32	60	2.32	70
2.47	100	2.34	40	2.33	40	2.20	40	2.47	90	2.34	10	1.86	10	2.20	60
2.34	20	2.20	30	2.20	40	1.91	30	2.33	40	2.20	10	1.78	60	1.99	10
2.20	30	1.92	40	1.92	30	1.78	50	2.20	30	2.00	10	1.71	10	1.96	10
1.93	10	1.79	50	1.87	30	1.71	30	1.93	30	1.87	10	1.67	30	1.86	40
1.87	20	1.64	30	1.79	30	1.68	30	1.87	40	1.83	5	1.60	10	1.83	10
1.79	10	1.54	30	1.72	20	1.54	40	1.83	30	1.72	10	1.53	30	1.78	70
1.72	10	1.50	30	1.68	30			1.79	40	1.68	10	1.47	10	1.70	40
1.68	20	1.36	30	1.54	30			1.68	40	1.50	10			1.67	60
1.50	10			1.50	20			1.54	30	1.48	20			1.60	30
1.46	20			1.48	20					1.24	10			1.54	70
1.24	20													1.47	60

[a] Reference 25. [b] Reference 24.

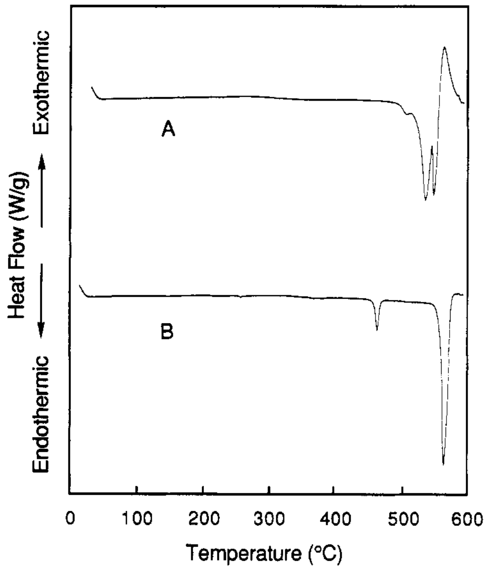

Figure 2. Differential scanning calorimetry curves for SVO samples measured under a purge of Ar gas. A heating rate of 20 °C/min and an argon purge rate of 120 mL/min were employed for the analysis: (A) $AgNO_3$ SVO synthesized under air; (B) $AgNO_3$ SVO synthesized under argon.

Table 3. X-ray Powder Diffraction Peaks (*d* Spacings, Intensities) for SVO Samples Prepared under an Argon Atmosphere

$AgNO_3$ SVO		Ag_2O SVO		$Ag_2V_4O_{11-y}$[a]	
d (Å)	int	*d* (Å)	int	*d* (Å)	int
7.02	10	7.10	50	7.10	30
3.93	20	6.02	40	5.40	30
3.54	90	3.90	40	3.94	80
3.44	10	3.53	50	3.48	70
3.12	40	3.44	80	3.08	100
3.03	100	3.12	90	3.05	30
2.98	10	3.05	90	2.98	50
2.65	10	3.02	100	2.71	70
2.59	10	2.98	70	2.59	40
2.36	70	2.64	40	2.54	30
2.03	20	2.58	60	2.51	10
1.98	10	2.37	40	2.42	40
1.92	10	2.33	30	2.325	70
1.80	10	2.03	40	2.260	60
1.74	10	1.80	50	2.165	30
1.55	10	1.74	40	2.043	60
1.52	10	1.60	30	1.940	30
1.46	10	1.55	40	1.798	80
1.36	20	1.52	30		
1.29	10	1.45	40		
		1.36	30		
		1.29	20		

[a] Reference 24.

displayed in Figure 2. Both samples display a small, sharp endothermic transition at 465 °C and a more intense endotherm at 569 °C. The appearance of an endotherm at 465 °C indicates that the samples may contain some $AgVO_3$ impurity, since $AgV_2O_{5.5}$ is known to form a eutectic with $AgVO_3$ which melts at 463 °C.[21] These results suggest that the SVO materials prepared under an oxidizing air atmosphere are more homogeneous than the samples prepared under argon.

X-ray powder diffraction analysis of the SVO samples was conducted on the as-synthesized materials to further characterize the samples. The data from these experiments are tabulated in Tables 2 and 3, and the powder patterns are presented in Figures 3 and 4. The crystalline powder samples synthesized under an air atmosphere all displayed the same *d* spacings, which correspond to the values listed for $AgV_2O_{5.5}$.[24,25] This indicates that all of the samples possess the same structure, matching the structure reported for SVO in the literature. However, the peak intensities varied depending on the choice of silver-containing precursor. A comparison of the ratio of integrated intensities for the most intense peak compared to the Si internal standard is given in Table 4. The difference in intensity ratios suggests that the Ag^0 SVO material possesses the highest degree of crystallinity of the samples, followed by SVO prepared from $AgNO_3$ and Ag_2CO_3. The remaining materials all displayed similar peak intensity ratios. In addition to the difference in overall peak intensity, the relative peak intensities also vary as a function of silver starting material. As can be seen in Figure 3 and Table 2, the peaks at *d* spacing of 7.36, 3.70, 2.47, 1.48, and 1.24 Å in the Ag^0 SVO sample are increased relative to the remaining peaks in the pattern when compared to the other SVO samples. The variation in relative peak intensities is most likely due to the

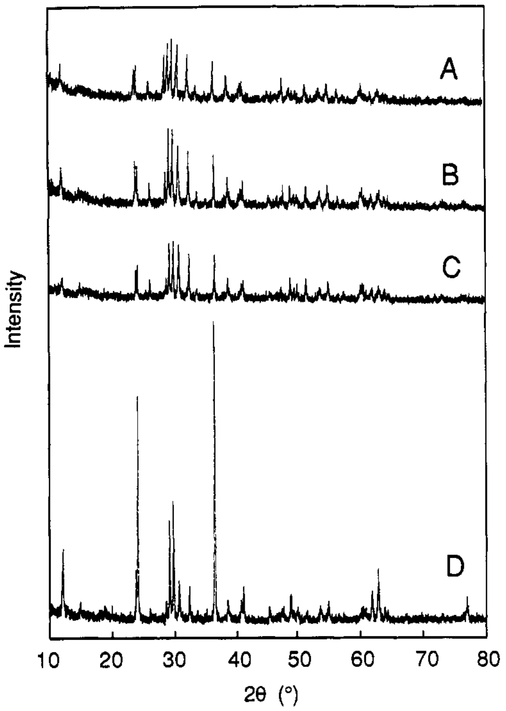

Figure 3. X-ray powder diffraction patterns of SVO samples recorded using Cu Kα radiation. Samples synthesized at 500 °C under an air atmosphere, from the reaction of V_2O_5 with (A) $AgNO_2$, (B) $AgVO_3$, (C) Ag_2CO_3, and (D) Ag^0 powder.

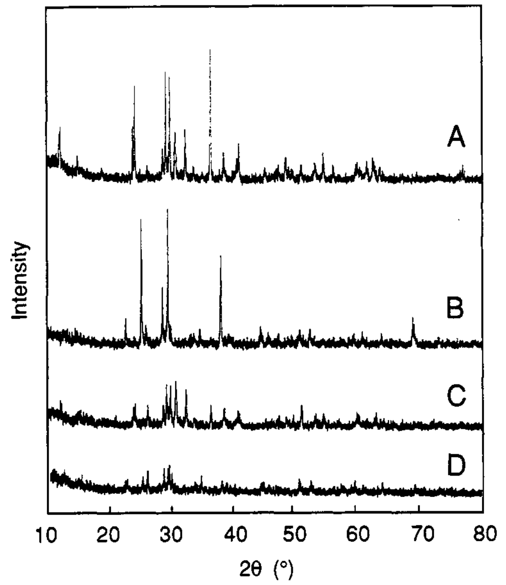

Figure 4. X-ray powder diffraction patterns of SVO samples recorded using Cu Kα radiation. Samples synthesized at 500 °C, from the reaction of V_2O_5 with (A) $AgNO_3$ under air, (B) $AgNO_3$ under argon, (C) Ag_2O under air, and (D) Ag_2O under argon.

Table 4. Integrated Intensity Ratios for X-ray Powder Diffraction of SVO Samples

SVO sample	synthesis atmosphere	peak ratio (most intense peak/ Si standard)
$AgNO_3$ SVO	air	6.6
$AgNO_2$ SVO	air	2.1
$AgVO_3$ SVO	air	3.1
Ag_2O SVO	air	2.7
Ag_2CO_3 SVO	air	4.9
Ag metal powder SVO	air	10.2
$AgNO_3$ SVO	argon	2.5
Ag_2O SVO	argon	1.2

Table 5. Resistivity Values for SVO Plates Pressed at 5400 kg/cm^2 and Sintered at 500 °C

SVO sample	synthesis/ sinter atmosphere	resistivity (Ω cm)
SVO from $AgNO_3$	air	39
SVO from $AgNO_2$	air	69
SVO from $AgVO_3$	air	58
SVO from Ag_2O	air	74
SVO from Ag_2CO_3	air	58
SVO from Ag^0 powder	air	56
SVO from $AgNO_3$	argon	1.1
SVO from Ag_2O	argon	0.8

difference in particle size and shape between the SVO materials,[39] as seen in Figure 1. As evidence of this, grinding of the Ag^0 SVO sample to reduce the particle size resulted in an X-ray powder pattern matching that obtained for the SVO sample prepared from $AgNO_3$. However, the difference in relative peak intensities between the as-synthesized materials was found to be reproducible for X-ray powder patterns recorded for duplicate preparations of SVO from $AgNO_3$ and Ag_2O. Thus the crystallinity of SVO samples prepared under air at 500 °C for a set time period appears to depend on the choice of silver-containing precursor.

The X-ray powder patterns for SVO samples prepared from $AgNO_3$ and Ag_2O under an argon atmosphere are displayed in Figure 4 along with the traces from the respective samples prepared under an air atmosphere. The *d* spacings and relative intensity data are given for the argon samples in Table 3, along with the standard data for $Ag_2V_4O_{11-y}$, an oxygen deficient form of SVO.[24] The samples prepared under argon display powder patterns quite distinct from the materials synthesized under air, indicating a different structure for the argon samples. In fact, the patterns resemble the oxygen deficient form of SVO, rather than $AgV_2O_{5.5}$. In addition, the presence of silver metal in the samples is suggested by the appearance of peaks at 2.36, 2.03, and 1.45 Å. The peak intensity ratio for the 2.36 Å silver metal peak and the Si standard were compared to the X-ray results for a known amount of silver metal powder added to a mixture of SVO and Si. On the basis of the intensities of the signals in the argon SVO samples, the percentage of silver in the reduced state is calculated to be 17% for the $AgNO_3$ sample, and 6% for the Ag_2O based material. Additionally, the signal intensities for the $AgNO_3$ SVO argon sample are much greater than those recorded for the sample from Ag_2O (Table 4). This suggests that the $AgNO_3$ sample is more crystalline than the sample from Ag_2O, a trend seen in the samples produced under an air atmosphere.

The conductivity of the samples was analyzed via resistivity measurements of pressed plates of SVO, with the results given in Table 5. The plates were all sintered at 500 °C, with the sinter atmosphere matching the atmosphere used in the synthesis of the materials. The SVO samples prepared under air all provided similar resistivity values, consistent with previous measurements of SVO prepared near this temperature.[36] A significant difference in resistivity was found for the SVO samples prepared under argon, where both the $AgNO_3$ and Ag_2O samples provided significantly lower resistivity than the corresponding samples prepared under air. The decrease in resistance may be due in part to the presence of conductive elemental silver in the samples, as suggested

---

[39] Cullity, B. D. *Elements of X-Ray Diffraction*, 2nd ed.; Addison-Wesley: Reading, MA, 1978; p 166.

Table 6. Chemical Analyses of Silver Vanadium Oxide Materials

SVO sample	synthesis atmosphere	% V^{4+}	% V^{5+}	empirical formula[a]
SVO from $AgNO_3$	air	1	99	$AgV_2O_{5.49}$
SVO from $AgNO_2$	air	2	98	$AgV_2O_{5.48}$
SVO from $AgVO_3$	air	2	98	$AgV_2O_{5.48}$
SVO from Ag_2O	air	2	98	$AgV_2O_{5.48}$
SVO from Ag_2CO_3	air	2	98	$AgV_2O_{5.48}$
SVO from Ag^0 powder	air	2	98	$AgV_2O_{5.48}$
SVO from $AgNO_3$	argon	13	87	$AgV_2O_{5.28}$
SVO from Ag_2O	argon	14	86	$AgV_2O_{5.33}$

[a] The emperical formulas calculated for the SVO samples prepared under an argon atmosphere take into account the presence of reduced silver observed in the X-ray powder diffraction experiment. The amount of reduced silver in these samples is estimated at 17% for $AgNO_3$ SVO and 6% for the Ag_2O SVO sample.

Table 7. Experimental Capacities for Li/SVO Cells Containing 1 M $LiAsF_6$ PC/DME Electrolyte

SVO sample	synthesis atmosphere	experimental capacity			
		to +2.0 V cutoff		to +1.5 V cutoff	
		A h/kg	W h/kg	A h/kg	W h/kg
SVO from $AgNO_3$	air	248	609	272	648
SVO from $AgNO_2$	air	248	598	282	655
SVO from $AgVO_3$	air	249	604	280	655
SVO from Ag_2O	air	253	618	282	666
SVO from Ag_2CO_3	air	252	614	280	660
SVO from Ag^0 powder	air	242	590	262	623
SVO from $AgNO_3$	argon	202	485	221	515
SVO from Ag_2O	argon	223	538	241	567

by the X-ray powder diffraction analysis. However, studies of SVO containing added silver metal powder showed that this amount of metallic silver could only account for ~10% of the increase in conductivity observed in the argon SVO samples. This suggests that the structural and compositional differences in these samples, evidenced by the X-ray powder diffraction and DSC data, play a larger role in determining the conductivity of the materials. Likewise, the lower resistivity of these species is in agreement with the resistivity values reported for the β and δ phases of SVO prepared under an inert atmosphere, where β-$Ag_{0.40}V_2O_5$ and δ-$Ag_{0.80}V_2O_5$ gave resistivity values of 3 and 1 Ω cm at 25 °C, respectively.[32,40]

Chemical analysis of the SVO materials provided information on the oxidation states of the vanadium components. The respective percentages of vanadium(IV) and vanadium(V) present in the SVO samples are listed in Table 6, along with the empirical formulas calculated for these species. The SVO samples synthesized under air contained primarily vanadium(V), with only a small amount (1–2%) of vanadium(IV). However, the samples prepared under an argon atmosphere contained considerably more vanadium(IV), at 13–14% of the entire vanadium content. The empirical formulas presented for the argon samples in Table 6 also take into account the presence of reduced silver metal, as determined by X-ray powder diffraction. The increased amount of vanadium(IV) in the argon samples suggests that this species is normally formed during the synthesis of SVO. However, when the synthesis is performed in the presence of air, the vanadium(IV) is reoxidized to vanadium(V) by reaction with oxygen at 500 °C.

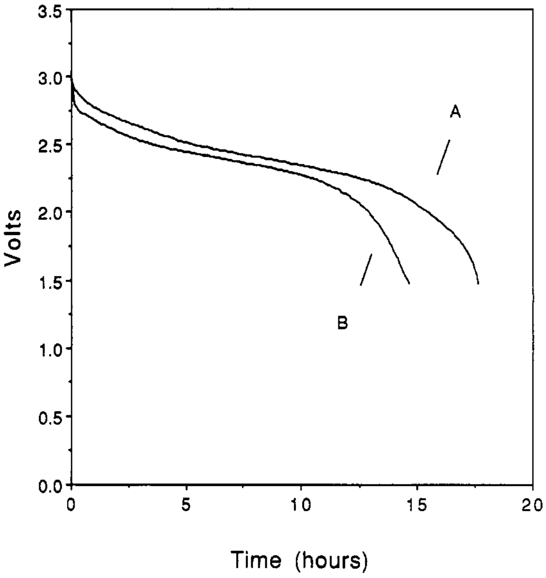

Figure 5. Constant resistance (200 Ω) discharge of Li/SVO in 1 M $LiAsF_6$ 50/50 by volume propylene carbonate/dimethoxyethane electrolyte at 25 °C: (A) $AgNO_3$ SVO synthesized under air; (B) $AgNO_3$ SVO synthesized under argon.

The electrochemical properties of the SVO samples were examined to determine the ability of these materials to act as cathodes in lithium batteries. Test cells were assembled using SVO cathodes, with lithium anodes and organic electrolyte. These cells were discharged under constant resistance loads at room temperature, and the capacities of the SVO samples were calculated on a per weight basis. Excess lithium and electrolyte were used in the cells, so that capacity was limited by the cathode material. The experimental capacity results are listed in Table 7. An experimental capacity of 280 A h/kg corresponds to the incorporation of 3.1 equiv Li into the $AgV_2O_{5.5}$ network. From Table 7 it is apparent that nearly all of the SVO samples prepared under an air atmosphere at 500 °C delivered the same amount of capacity. In addition, no difference was found in the shape of the voltage vs time curves for these samples. The sample prepared from silver metal powder provided slightly lower capacity to a +2.0 and +1.5 V cutoff, as seen in Table 7. However, the use of the SVO samples prepared under an argon atmosphere resulted in a significant decrease in delivered capacity. A 19% decrease in capacity was found for $AgNO_3$ SVO prepared under argon versus material prepared under air. Likewise a 14% decrease was found for Ag_2O SVO from argon relative to air. A comparison of the voltage versus time discharge curves for Li/SVO cells containing $AgNO_3$ SVO from argon and air atmospheres is displayed in Figure 5. While the synthesis of SVO under an inert atmosphere produces a cathode material with lower overall capacity, the amount of vanadium(IV) detected in the chemical analysis of the argon SVO samples (Table 6) does not completely account for this decrease in capacity. The loss in capacity due to vanadium(IV) is calculated at 5% for the $AgNO_3$ sample, and 6% of the Ag_2O sample from the chemical analysis data, leaving 14% and 8% of unaccounted capacity loss, respectively. Part of the remaining shortfall in capacity is likely due to the presence of reduced silver in the samples, as noted in the X-ray analysis of the materials. During the normal discharge of SVO, Ag^+ is reduced to Ag^0, and V^{5+} is reduced to V^{4+} and then V^{3+}. Thus, the presence of reduced silver in the starting SVO material would lower the overall capacity of the cathode material. The amount of capacity lost due to silver metal in the samples

---

(40) Casalot, A.; Cazemajor, H.; Hagenmuller, P.; Pouchard, M.; Roch, J. *Bull. Soc. Chim. Fr.* **1968**, 85–90.

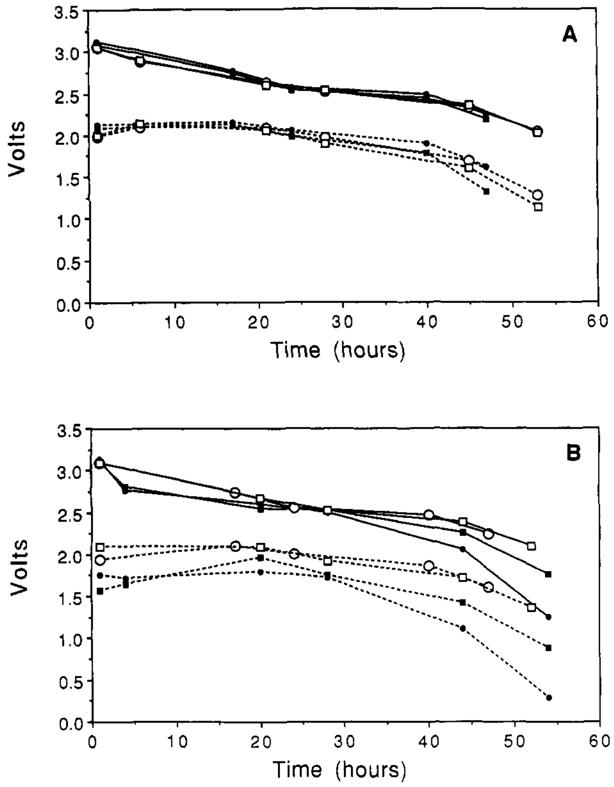

Figure 6. Pulse power capability of Li/SVO cells containing 1 M $LiAsF_6$ 50/50 by volume propylene carbonate/dimethoxyethane electrolyte at 25 °C. The background voltages of the cells prior to pulse appear in the upper traces (—) and the minimum cell voltages during the application of the pulse current appear in the lower traces (- - -). (A) (○) $AgNO_2$ SVO, (□) $AgVO_3$ SVO, (●) Ag_2CO_3 SVO, (■) Ag^0 powder SVO. (B) (○) $AgNO_3$ SVO (air), (□) Ag_2O SVO (air), (●) $AgNO_3$ SVO (argon), (■) Ag_2O SVO (argon).

(estimated from the X-ray powder diffraction data) is calculated at 3.5% for the $AgNO_3$ sample and 1% for the Ag_2O sample. The balance of capacity difference between the air and argon SVO samples may be due to a difference in structure and composition between the materials, affecting the amount of lithium that can be incorporated in the samples.

In addition to studying the constant resistance discharge of the SVO cathode materials, a high-rate pulse discharge of the cells was undertaken. The pulse discharge test was employed to determine the ability of the cathode materials to withstand a heavy discharge load, an important function of Li/SVO batteries. Li/SVO test cells were assembled as before and placed on a low-rate constant resistance load. The cells were then subjected to a set of four constant-current pulses twice a day until the cell background voltage reached +1.5 V. The background voltages and minimum pulse voltages are plotted for the cells in Figure 6. The upper traces in this figure represent the background voltage values and the lower traces represent the minimum voltages measured while a pulse current was applied to the cell. The difference between these two voltage readings is tabulated as an average for each cell in Table 8. Note from Table 8 and Figure 5 that all of the SVO cathode materials prepared under an air atmosphere provided nearly identical results. This indicates that the electrochemical properties of the SVO material are virtually independent of the choice of silver-containing precursor used in this study, as long as the synthesis conditions are held constant. An earlier study demonstrated that the capacity of SVO cathode material will change significantly if the temperature of preparation is varied.[36] While the SVO materials produced under an air atmosphere all provided similar electrochemical results, they are significantly different from the results measured for the SVO samples prepared under an argon atmosphere (Table 8). These tests indicate that the samples prepared under an air atmosphere provide a higher pulse power capability than the samples synthesized under argon.

Table 8. Pulse Power Capability of Li/SVO Cells Containing 1 M $LiAsF_6$ PC/DME Electrolyte

SVO sample	synthesis atmosphere	average ΔmV,[a] mV
SVO from $AgNO_3$	air	720
SVO from $AgNO_2$	air	720
SVO from $AgVO_3$	air	760
SVO from Ag_2O	air	720
SVO from Ag_2CO_3	air	660
SVO from Ag^0 powder	air	740
SVO from $AgNO_3$	argon	990
SVO from Ag_2O	argon	960

[a] ΔmV = drop in voltage with application of pulse current to the cell = background voltage − minimum pulse voltage.

Conclusions

The synthesis of silver vanadium oxide at 500 °C and under an air atmosphere produced samples with similar particle shapes, although the overall particle sizes varied with respect to silver source. Thermal analysis of the products indicated an identical composition for all of the materials, corresponding to $AgV_2O_{5.5}$. Likewise, resistivity measurements of pressed plates provided very similar values for the SVO materials. However, the X-ray powder diffraction patterns for the samples showed some important differences in the crystallinity of the materials. While the samples all displayed the same peaks, indicating identical structures, the peak intensities varied significantly depending on the silver-containing precursor used in the reaction. In particular, the results suggest that the SVO sample produced from silver metal powder is more crystalline than the other samples. The electrochemical properties of the materials were examined in Li/SVO nonaqueous test cells, and the difference in crystallinity of the samples did not produce a large difference in delivered capacity in the cells. However, the sample produced from silver metal provided the lowest delivered capacity, suggesting that highly crystalline forms of SVO may display reduced capacity. In addition, the ability of the Li/SVO test cells to provide high pulse power showed no difference between the SVO samples, suggesting that crystallinity plays little, if any, role in determining the pulse power capability of the SVO cathode material.

While varying the silver-containing precursor had apparently little effect on the final SVO product, changing the synthesis atmosphere to argon produced very different materials. Results from SEM, DSC, chemical analysis, X-ray powder diffraction, and resistivity measurements were all very different from those obtained for the samples produced under air. The difference in the argon materials was also reflected in the experimental capacity and pulse power capability of the Li/SVO cells, where the argon samples provided significantly decreased electrical performance relative to the air samples. The decrease in capacity for the argon cells appears to be due to a significant amount of vanadium(IV) and reduced silver metal in the samples. Thus, the presence of air in the preparation of SVO at 500 °C acts to reoxidize any reduced components of SVO formed during the synthesis reaction.